Journal of
Polymer Materials

Tech Science Press

http://doi.org/10.32604/jpm.2026.087801

ARTICLE

Bio-Based Vitrimer Foam of Bis-Glycidyl Dehydroabietylamine/Epoxidized Soybean Oil with Self-Healing and Shape Memory Properties

Wenxuan Zhang[1], Zhengchuang Zhao[1], Xiaoting Gao[1], Wenning Shen[2], Ruiqin Deng[1], Zheng Xing[1], Huimin Cheng[1] and Xinyan Yan[1,*]

[1]School of Chemistry & Chemical Engineering, Yancheng Institute of Technology, Yancheng, China
[2]Nanxun Branch of Huzhou Municipal Bureau of Ecology and Environment, Huzhou, China
*Corresponding Author: Xinyan Yan. Email: 18752008824@163.com

Received: 23 June 2026; Accepted: 26 August 2026; Published: 24 September 2026

ABSTRACT: High bio-based polymer foams face a critical challenge in balancing mechanical robustness with re-processability and environmental sustainability. In this work, a novel bio-based vitrimer foam was fabricated by integrating rigid rosin-derived Bis-glycidyl dehydroabietylamine epoxy resin (DGDHAA) with flexible epoxidized soybean oil (ESO) within a dynamic covalent network. Sodium bicarbonate served as the foaming agent, N,N-dimethylbenzylamine as the foam stabilizer, triethanolamine as the catalyst, and bis(3-aminopropyl) amine (BAPA) as both the curing agent and reactive diluent. The resulting DGDHAA/ESO-BAPA foams exhibited tunable glass transition temperatures (T_g) ranging from 95.88°C to 98.65°C with increasing BAPA content, along with excellent thermal stability. The optimized formulation achieved a compression resilience of 81.84%, demonstrating outstanding elastic recovery. Moreover, the foams displayed remarkable shape-memory behavior and self-healing capability: after thermal treatment at 120°C for 2 h, the healed specimen could sustain a hanging load of 500 g without fracture. This work demonstrates that the rational combination of rigid rosin-based skeletons and flexible vegetable oil chains within a dynamic covalent network provides an effective strategy for developing high-performance, high bio-based foams with tunable thermal properties, excellent elasticity, self-healing ability, and environmental compatibility.

KEYWORDS: Bis-glycidyl dehydroabietylamine; epoxidized soybean oil; thermosetting foams; shape memory; self-healing

1 Introduction

Epoxy resin foams are widely used in packaging, buffering, aerospace, energy conservation and environmental protection and other fields due to their characteristics of low density, heat insulation and excellent mechanical properties. However, conventional epoxy foams are intrinsically non-reprocessable owing to their permanently cross-linked network structure, which also brings about poor degradability and subsequent environmental disposal dilemmas [1].

With the rapid advancement of dynamic covalent chemistry, dynamic covalent networks have emerged as a promising solution to address the challenges of recyclability, reparability, and reprocessability of thermosetting foams [2,3]. Epoxy vitrimer foams constructed via dynamic ester bonds, imine bonds, or disulfide bonds can undergo topological network rearrangement under thermal, aqueous, or mild chemical stimuli. These materials combine the excellent stability of conventional thermosets with the reprocessability of thermoplastics, and can also be degraded and recovered under mild conditions. Jing et al. [4] introduced

acid-base ionic pairs into a dense and robust hydrogen-bonding network, and constructed rigid self-healing supramolecular polymers with tunable stiffness and outstanding toughness via dynamic noncovalent interactions. However, despite these advantages, most existing epoxy vitrimer foams still rely heavily on petroleum-based resources, which poses a significant limitation to their long-term sustainability and environmental compatibility [5–8].

Against the backdrop of escalating environmental pollution and the depletion of petroleum resources, the concepts of green chemistry and sustainable polymer development have gained increasing prominence. Bio-based thermosetting foams, derived from renewable biomass resources, offer notable advantages including abundant raw material sources, low carbon footprint, environmental friendliness, ease of repair, and inherent degradability, positioning them as promising candidates to replace petroleum-based materials [9]. In recent years, various bio-based feedstocks—such as soybean oil, linseed oil-derived epoxy monomers—have been successfully employed in the fabrication of epoxy foams, with significant progress achieved in density regulation, pore structure optimization, and thermal performance enhancement. For instance, Altuna et al. [10] prepared thermosetting epoxy foams with high bio-based content using epoxidized soybean oil (ESO) and methyltetrahydrophthalic anhydride (MTHPA) as the main components and $NaHCO_3$ as the blowing agent. The resulting foams exhibited tunable density and satisfactory mechanical properties. However, they suffered from a low glass-transition temperature (T_g) and inadequate heat resistance. Moreover, excessive foaming agent led to limited density reduction and a decrease in crosslinking density. Similarly, Tanrattanakul et al. [11] developed a flexible bio-based epoxy foam by reinforcing epoxidized soybean oil with epoxidized mangosteen tannin (EMT), using azodicarbonamide/ZnO as the foaming agent. The foam showed enhanced compressive strength and reduced compression set, while its subzero T_g and mixed open/closed cell structure confirmed its flexible nature. Despite being more environmentally friendly than petroleum-derived epoxy resins, bio-based epoxy systems are generally constrained by insufficient mechanical properties, which severely limits their widespread practical application. Employing rigid biomass resources can effectively address this issue by imparting enhanced stiffness, thermal stability, and structural integrity to the foam matrix.

Rosin is a natural resin derived from pine trees. As one of the most important modified derivatives of rosin, dehydroabietylamine contains a rigid hydrogenated phenanthrene ring skeleton in its molecular structure, which not only endows it with excellent thermal stability and mechanical strength but also good chemical reactivity. This unique structural feature enables rosin and its modified products to exhibit enormous application potential in various polymer material fields, including epoxy resins [12,13], coatings [14–16], and adhesives [17]. The high mechanical strength of petroleum-based epoxy resins, typically represented by bisphenol A type, is mainly attributed to the rigid effect of benzene rings in their molecular structures. In contrast, the inherent tricyclic phenanthrene skeleton (i.e., hydrogenated phenanthrene ring) of dehydroabietylamine, as a rigid cyclic structure, has a highly similar configuration and stable molecular structure to the aromatic or alicyclic compounds in petroleum-based epoxy resins. It can effectively replace the rigid structural units in bisphenol A molecules, thereby significantly enhancing the mechanical strength and thermal stability of composite materials [18,19]. A large number of studies have confirmed that the introduction of rosin-based rigid structures into epoxy resin polymer systems can effectively improve the mechanical properties, thermal stability, and T_g of thermosetting resins which further validates the application value of rosin and its modified products in epoxy resin modification [20–22]. Tian et al. [23] prepared a fully bio-based degradable vitrimer foam (EPC-X) by an integrated foaming process using rosin-based epoxidized maleopimaric anhydride (EMPA) and 1,5-pentanediamine (PDA) as the main components, and pentanediamine carbamate (PDAC) as a latent curing-foaming bifunctional agent and the obtained material

displayed favourable mechanical performances. Huang et al. [24] prepared bio-based thermosetting epoxy foams using ESO and rosin derivative fumaropimaric acid (FPA) as raw materials and $NaHCO_3$ as the foaming agent. With the increase of FPA content, the apparent density of the foam decreases, the porosity increases, and the thermal stability is excellent, showing potential to replace petroleum-based epoxy foams. Moreover, bio-based epoxy resins such as rosin-based and vegetable oil-based resins, with their unique rigid skeletons and flexible long-chain structures, provide ideal raw materials for constructing high-performance dynamically cross-linked foam [25–27]. At present, the research on constructing bio-based vitrimer foams by compounding rosin-based epoxy resins with vegetable oil-based epoxies and using dynamic amine curing agents is still relatively limited. Bio-based foaming systems that balance thermal stability, high resilience, shape memory and self-healing multifunctions are urgently needed to be developed.

In terms of foaming technology, green volatile organic compound (VOC)-free foaming systems such as carbon dioxide latent foaming agents [28–30], $NaHCO_3$ [31,32] and carbamates [33,34] have gradually replaced traditional harmful foaming agents, realizing one-step synchronous foaming and curing, which significantly simplifies the process and improves the uniformity and stability of foams. Chen et al. [35] fabricated biodegradable starch-based polyether NIPU foams using sodium bicarbonate and silane coupling agent KH560 as the foaming system. The resulting foams possessed low thermal conductivity and tailorable compressive strength. BAPA has a small molecular volume and contains 5 active hydrogen atoms (derived from two terminal primary amines and one middle secondary amine), which can rapidly undergo nucleophilic ring-opening polymerization with the epoxy groups in epoxy resins [36]. Moreover, BAPA is a low-viscosity liquid; when used as a curing agent in the curing reaction of epoxy resins, it can not only significantly reduce the overall viscosity of the system but also exert a certain diluting effect. This is crucial for formulating solvent-free or high-solid-content environmentally friendly epoxy resin systems, as it can provide excellent leveling property and wettability to the substrate for the reaction [37].

Based on this, this study prepared a new type of bis-glycidyl dehydroabietylamine/epoxidized soybean oil-based bis(3-aminopropyl) amine bio-based vitrimer foam using DGDHAA as the rigid matrix, ESO as the flexible component, BAPA as the dynamic curing agent, $NaHCO_3$ as the foaming agent, BDMA as the foam stabilizer, and TEOA as the catalyst. By regulating the dosage of curing agent BAPA, the effects of BAPA on the microstructure, thermal properties and mechanical properties of the foam were systematically investigated, and the shape memory and self-healing behaviors of the material were deeply analyzed. The purpose is to develop a green, environmentally friendly and multi-functional integrated bio-based dynamically cross-linked foam, and provide experimental basis and theoretical reference for the design and application of high-performance bio-based thermosetting foaming materials.

2 Experimental

2.1 Materials

Dehydroabietylamine (DHAA, 98%) was supplied by Xuancheng Jingrui New Materials Co., Ltd. Epichlorohydrin (ECH) was purchased from Shanghai Yansu Technology Co., Ltd. Tetrabutylammonium bromide (TBAB, 99%) was provided by Saan Chemical Technology (Shanghai) Co., Ltd. Anhydrous magnesium sulfate was obtained from Shanghai Pilot Chemical General Company. Petroleum ether was purchased from Shanghai Lingfeng Chemical Reagent Co., Ltd. Bis(3-aminopropyl) amine (BAPA, 98%) was supplied by Shanghai Yuanye Biotechnology Co., Ltd. $NaHCO_3$ was provided by Yonghua Chemical Technology (Jiangsu) Co., Ltd., N,N-dimethylbenzylamine (BDMA, 99%) and epoxidized soybean oil (ESO) were purchased from Shanghai Macklin Biochemical Technology Co., Ltd., while NaOH and triethanolamine (TEOA) were obtained from Jiangsu Tongsheng Chemical Reagent Co., Ltd. All experimental water was distilled water.

2.2 Preparation of Bis-Glycidyl Dehydroabietylamine Epoxy Monomer (DGDHAA)

In this work, a bis-glycidyl dehydroabietylamine epoxy monomer (DGDHAA) was synthesized using dehydroabietylamine (DHAA) and epichlorohydrin as raw materials, and the corresponding synthetic route is displayed in Fig. 1A. To achieve high conversion efficiency and obtain high-purity monomer products, the reaction parameters and purification procedures were precisely optimized in this study. The detailed synthetic procedures are described as follows: 57 g of dehydroabietylamine (DHAA) was mixed with 223.2 g of excess epichlorohydrin (ECH), followed by the addition of 10 mL of water. The mixture was placed in a constant-temperature oil bath at 45°C for continuous low-temperature stirring reaction for 150 h. Tetrabutylammonium bromide (TBAB) was added to the system as a catalyst, and then a 15% (mass fraction) aqueous NaOH solution was slowly added dropwise. The stirring reaction was continued under constant temperature conditions for 3 h to allow the intermediate to remove hydrogen chloride in an alkaline environment and complete the ring closure of terminal epoxy groups. After the reaction, the precipitated chloride salt solids in the system were removed by suction filtration. After collecting the filtrate, an appropriate amount of anhydrous magnesium sulfate was added and allowed to stand for a period of time to adsorb residual water, and then the magnesium sulfate was removed by filtration. The obtained organic phase was extracted and washed with petroleum ether, and the unreacted raw materials and low-polarity impurities were separated and removed from the product by virtue of the selective solubility of petroleum ether for non-polar components. The purified product was placed in a vacuum oven and dried to constant weight at 90°C to obtain the target product DGDHAA. The epoxy value of DGDHAA was determined to be 0.47 mol/100 g by the perchloric acid titration method, and the theoretical value was 0.49 mol/100 g, reaching 95.91% of the theoretical value. The synthetic route of DGDHAA is shown in Fig. 1.

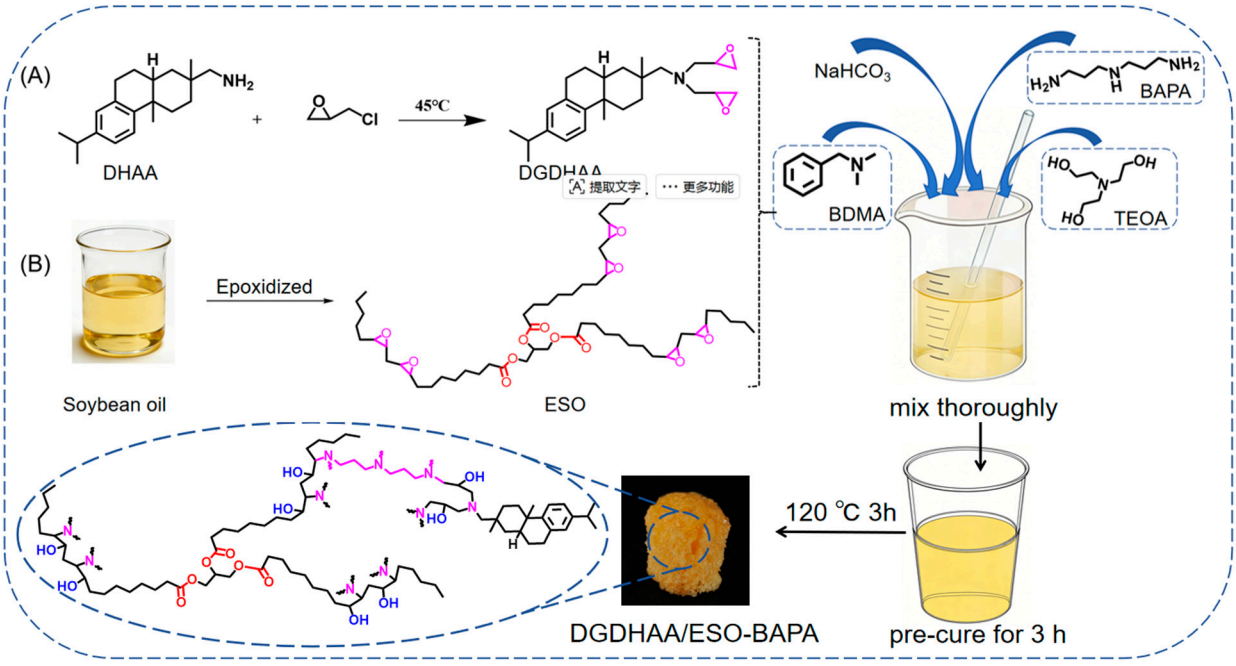

Figure 1: Synthetic route of DGDHAA and the process of preparing the foam.

2.3 Preparation of Bis-Glycidyl Dehydroabietylamine/Epoxidized Soybean Oil-Based Bis(3-Aminopropyl) Amine Bio-Based Vitrimer Foam—DGDHAA/ESO-BAPA

To investigate the effect of the epoxy-to-amino molar ratio on the properties of the vitrimer foam, the DGDHAA/ESO mass ratio was kept constant, and only the amount of curing agent BAPA was varied. Three formulations were designed with epoxy/BAPA molar ratios of 1:0.8, 1:1.0, and 1:1.2 and designated as DGDHAA/ESO-BAPA 0.8, DGDHAA/ESO-BAPA 1.0, and DGDHAA/ESO-BAPA 1.2, respectively. The completed curing formulation is summarized in Table 1. Triethanolamine (TEOA) was used as the catalyst, with a fixed addition of 0.03 g in all formulations. The mixture was stirred thoroughly to ensure complete homogenization of DGDHAA, epoxidized soybean oil, and $NaHCO_3$.

Take DGDHAA/ESO-BAPA 1.0 as an example: according to a DGDHAA-to-ESO mass ratio of 2:1, 1.5 g of DGDHAA, 0.75 g of ESO, and 20 wt% $NaHCO_3$ (relative to the total resin mass) were weighed and placed in a beaker. Subsequently, 0.061 g of BDMA, 0.03 g of TEOA, and 0.265 g of BAPA were added and mixed evenly. The resulting mixture was poured into a cup-shaped mold and allowed to pre-cure at room temperature for 3 h.

After pre-curing, the foam was transferred to an oven at 120°C for simultaneous curing and foaming for 3 h. Upon completion of the reaction, the foam was demolded while still hot to preserve its structural integrity. Finally, a high bio-based vitrimer foam based on DGDHAA, ESO, and BAPA was successfully obtained.

Table 1: Curing formulation of the DGDHAA/ESO-BAPA system.

Samples	DGDHAA (g)	ESO (g)	BAPA (g)	BDMA (g)
DGDHAA/ESO-BAPA 0.8	1.5	0.75	0.212	0.060
DGDHAA/ESO-BAPA 1.0	1.5	0.75	0.265	0.061
DGDHAA/ESO-BAPA 1.2	1.5	0.75	0.318	0.063

2.4 Characterization

2.4.1 Product Structure Characterization

The Nicolet iS20 Fourier transform infrared (FT-IR) spectrometer was used to perform infrared testing on the product by the tablet pressing method, with a test wavenumber range of 500 cm^{-1}–4000 cm^{-1}. The ^{13}C NMR spectrum and ^{1}H NMR spectrum were measured using the AVANCE NEO 500 MHz nuclear magnetic resonance instrument, with deuterated chloroform as the solvent.

2.4.2 Thermogravimetric Analysis (TGA) and Glass Transition Temperature (T_g) Measurement

The thermal stability and glass transition temperature (T_g) of the samples were synchronously tested using a PerkinElmer STA 8000 simultaneous thermal analyzer. The test conditions were set as follows: the temperature range was 25–800°C, nitrogen was used as the protective gas, and the heating rate was 10°C/min.

2.4.3 Compressive Tests

A Wanyi WY-2000A testing machine was used for compressive tests. The test conditions were: a 5 kN sensor was used, and the compression test was performed at a rate of 5 mm/min.

2.4.4 Scanning Electron Microscopy

The cross-sectional morphology of the bio-based resin foams was analysed using scanning electron microscopy (SEM). The sample cross-sections were prepared by liquid nitrogen brittle fracture and sputter-coated with a gold layer to prevent charging effect during observation. SEM image with a 1 mm scale bar was captured to evaluate the porous architecture and cellular homogeneity of the foams, and ImageJ software was employed to quantitatively determine the pore size.

3 Results and Discussion

3.1 Structure Characterization

The structure of DGDHAA, synthesized via the reaction between DHAA and epichlorohydrin, was effectively characterized by FT-IR, ^{1}H NMR, and ^{13}C NMR spectroscopy. The corresponding spectra are presented in Figs. S1–S3. These results confirm the successful synthesis of the target bio-based epoxy resin prepolymer, DGDHAA.

The FTIR spectrum of the solidified bio-based vitrimer foam is shown in Fig. 2. From the spectrum, it can be seen that the characteristic peak of the epoxy group at 968 cm^{-1} of the cured product has significantly weakened, indicating that a large number of epoxy groups in the system have been consumed and participated in the ring-opening reaction. At the same time, the characteristic absorption peaks of the amino group corresponding to 3287 cm^{-1} and 1600 cm^{-1} of pure BAPA basically disappeared in the cured system, and the intensity of the N-H stretching vibration signal significantly weakened, and overlapped with the hydroxyl absorption peak. Moreover, a clear hydroxyl characteristic broad peak appeared at 3380 cm^{-1} in the product, indicating that the epoxy group and the amino group have undergone cross-linking reactions and generated a large number of hydroxyl structures. The evolution pattern of these characteristic peaks fully confirms that DGDHAA/ESO and BAPA successfully undergo epoxy-amino curing reaction, and successfully prepared DGDHAA/ESO-BAPA.

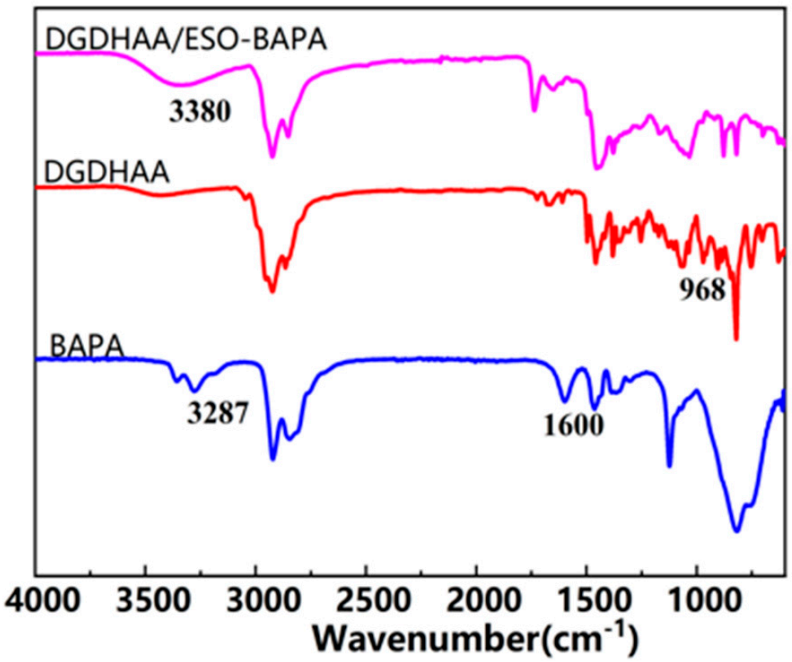

Figure 2: Infrared spectra of DGDHAA, BAPA and DGDHAA/ESO-BAPA.

3.2 TG Analysis

In the characterization of polymer materials, the thermal stability limit of samples directly determines the accuracy and reliability of high-temperature experimental test results [38]. In this work, thermogravimetric analysis (TGA) was adopted to systematically investigate the thermal decomposition behaviors of DGDHAA/ESO-BAPA foams with different BAPA curing agent contents, and the corresponding TG and DTG curves are presented in Fig. 3A,B, respectively. All samples exhibited no obvious mass loss from room temperature to 250°C. Only a weak low-temperature weight loss peak appeared at approximately 190°C, which corresponded to the thermal decomposition of unreacted small molecules in the system, including residual free diamines and trace foaming agent residues. The intensity of this low-temperature decomposition peak increased with the elevation of BAPA dosage, which was attributed to the increased content of free amine components in the system. The major thermal decomposition stage of the prepared foams occurred in the range of 250–400°C, and the mass loss in this stage was mainly caused by the cleavage of dynamic covalent bonds within the crosslinked network and the thermal degradation of the rigid tricyclic phenanthrene skeleton of a small amount of unreacted DGDHAA monomers. Samples with different BAPA contents displayed distinct thermal decomposition differences during this stage. The DGDHAA/ESO-BAPA 0.8 sample showed a relatively broad main weight loss peak, indicating a dispersed bond cleavage process caused by insufficient crosslinking density. The DGDHAA/ESO-BAPA 1.0 sample possessed the lowest peak temperature and the strongest peak intensity, revealing poor crosslinking network uniformity and inferior thermal stability. In contrast, the main decomposition peak of the DGDHAA/ESO-BAPA 1.2 sample shifted toward a higher temperature. This phenomenon demonstrated that an appropriate increase in BAPA content effectively improved the crosslinking density of the system and enhanced the thermal stability of the material, which partially offset the toughening and flexible effects brought by the flexible chains of ESO. The thermal decomposition of all samples was basically completed at 500°C. Benefiting from the inherent rigid skeleton structure of rosin, the fabricated bio-based vitrimer foams achieved prominently improved thermal resistance and exhibited excellent comprehensive thermal stability.

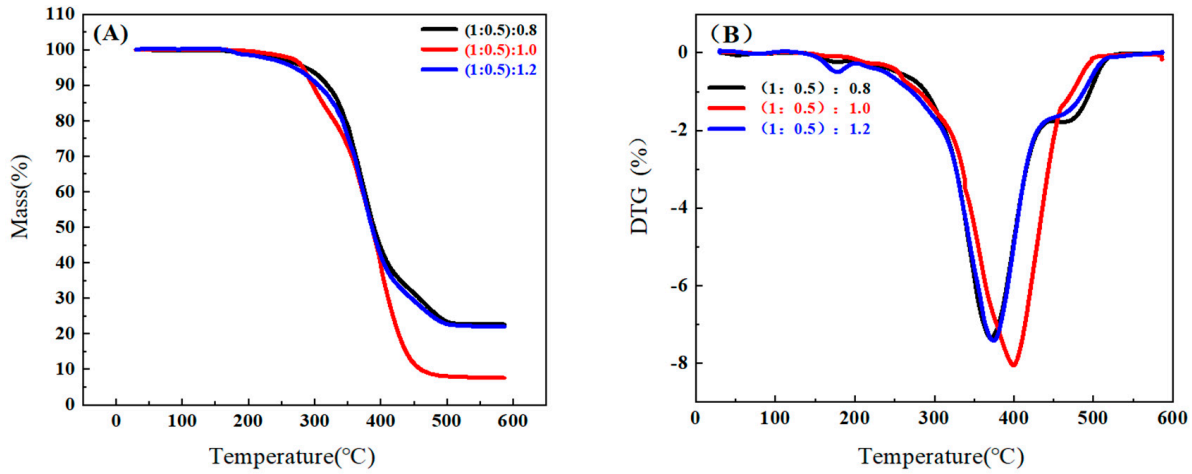

Figure 3: (**A**) Thermogravimetric curve of DGDHAA/ESO-BAPA; (**B**) DTG curve of DGDHAA/ESO-BAPA.

3.3 DSC Thermal Property Analysis

The glass transition temperature (T_g) can be determined using the midpoint method [39]. Specifically, tangents are drawn to the baseline in the glassy region (before transition) and the rubbery region (after

transition) of the DSC curve. T_g is determined as the temperature at the midpoint of the heat-capacity change between the extrapolated glassy and rubbery baselines. According to the DSC curves in Fig. 4, the T_g values of different formulations show a significant gradient increase: the T_g of the DGDHAA/ESO-BAPA 0.8 system is 95.88°C, rising to 96.53°C for the DGDHAA/ESO-BAPA 1.0 system; the highest T_g value is observed in the DGDHAA/ESO-BAPA 1.2 system, reaching 98.65°C. As the BAPA content increases, the crosslinking reaction between epoxy groups and amine groups becomes more complete, forming a denser three-dimensional crosslinked network. The increased density of crosslinking points significantly restricts local rotation and cooperative motion of polymer segments, while the tighter network structure reduces the free volume within the polymer matrix. Consequently, higher thermal activation energy is required for the transition from the glassy to the rubbery state, resulting macroscopically in a shift of T_g toward higher temperatures. Notably, although the flexible ESO chain segments enhance material toughness, the dominant effect is the increased rigidity caused by high crosslinking density, leading to an increase in T_g with increasing curing agent content. Experimental results indicate that by adjusting the ratio of DGDHAA/ESO to BAPA, the thermal resistance of the material can be effectively controlled-T_g increases with higher ratios, and the overall rigidity of the system improves. The thermoresponsive PDMAPS polymer developed by Su et al. [40] exhibits a phase transition temperature of merely 28–30°C, which triggers the switch of heat transfer regulation once the temperature rises slightly above room temperature. In contrast, benefiting from the synergistic effect between the rosin-based tricyclic phenanthrene rigid skeleton of DGDHAA and the dynamic crosslinking network formed by BAPA, the as-prepared foam achieves T_g ranging from 95.88 to 98.65°C, with no significant mass loss observed below 250°C.

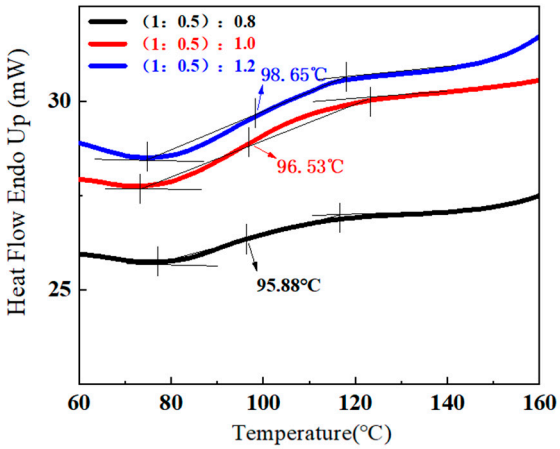

Figure 4: T_g of DGDHAA/ESO-BAPA.

3.4 Compressive Properties

The compression recovery performance of foam materials is one of the key indicators to evaluate their mechanical toughness and structural stability [41], and its test process and results are shown in Fig. 5. The figure records the instantaneous images of three key stages during the compression test: 0% loading (initial state), 50% loading (compression process) and after unloading (recovery state), which intuitively presents the compression-recovery process of vitrimer foams with different ratios. As shown in Fig. 5A, the DGDHAA/ESO-BAPA 1.0 sample exhibits excellent elastic recovery characteristics in the compression test: the initial height of the sample is 12.5 mm, and after undergoing 50% compressive deformation (i.e., the compression displacement is 6.25 mm), obvious rebound behavior occurs during the unloading process,

and the final recovery height can reach 10.23 mm, corresponding to a rebound rate as high as 81.84%. The sample only undergoes uniform elastic deformation during the compression stage, without obvious local crushing or cracks; after unloading, the foam structure almost recovers to its initial intact morphology, with only a small amount of micro-deformation traces left at the micro level due to the relaxation of the cross-linked network. In contrast, the compression recovery performance of the DGDHAA/ESO-BAPA 1.2 sample is reduced, as shown in Fig. 5B. The initial height of this sample is 14.5 mm, and under the same compression test conditions, the recovery height after unloading is only 8.4 mm, corresponding to a compression rebound rate of 57.93%. It is worth noting that the DGDHAA/ESO-BAPA 0.8 sample undergoes brittle fracture during the loading process and cannot complete the full compression recovery test. This phenomenon indicates that the low crosslinking density cannot provide sufficient mechanical support for the foam structure, and the material is prone to irreversible fracture damage when compressed. Compared with the rigid and ultra-tough intermolecular polymers reported by Jing et al. [4], the foam fabricated in this work achieves additional compressive properties owing to its porous microstructure. The compressive stress of the foam mainly depends on the properties of the bubble wall [42]. Due to the introduction of the hydrogenated phenanthrene ring structure of DHAA, the rigidity and strength of the bio-based vitrimer bubble wall have also increased. Therefore, with the increase of BAPA curing agent dosage, the compression recovery performance of this series of vitrimer foams shows a trend of first increasing and then decreasing.

In summary, DGDHAA/ESO-BAPA 1.0 exhibited the best overall performance; therefore, this composition was selected for subsequent investigations.

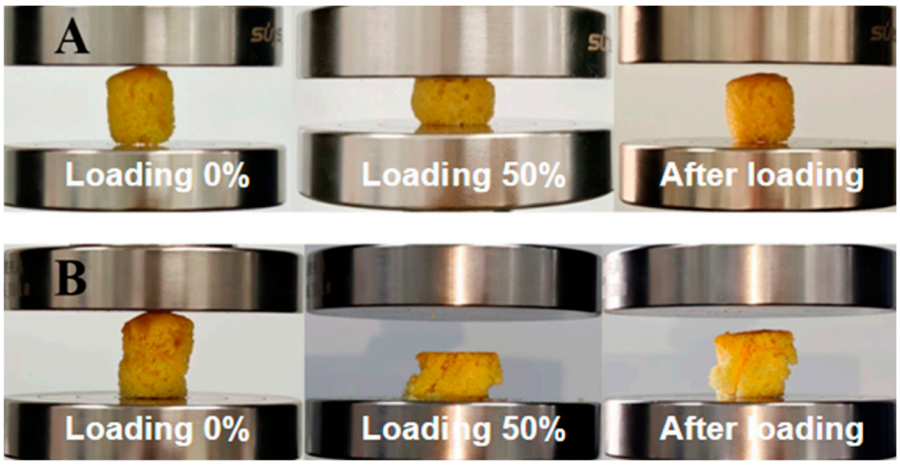

Figure 5: Compression test images of (**A**) DGDHAA/ESO-BAPA1.0 and (**B**) DGDHAA/ESO-BAPA1.2.

3.5 Shape Memory Properties

In the vitrimer material with hydroxy-ester dynamic covalent bonds, the thermally-triggered ester exchange reaction endows it with shape memory properties, enabling the cured material to be reshaped [43,44]. As shown in Fig. 6, the foam can achieve the "deformation → fixation → recovery" cycle because the curing agent BAPA undergoes ring-opening crosslinking reaction with DGDHAA and ESO to form a dense and stable three-dimensional covalent network. Place the foam sample at a temperature higher than T_g, and under the action of an external force, flatten or twist the foam into a temporary shape. After cooling to room temperature, remove the external force. The shape will not change. Reheat it to a temperature higher than T_g, and it will recover to its original form. When the foam is twisted into a temporary shape, full recovery of its original complete morphology can be achieved by heating at 120°C for only 1 min.

At 120°C, these covalent bonds remain stable, ensuring that the original topological structure is not destroyed. The long aliphatic flexible segments in ESO endow the cross-linked network with great free volume and segment mobility, enabling the foam to withstand large strains (such as being flattened or folded in half) without brittle fracture when heated. The tricyclic phenanthrene rigid skeleton in the DGDHAA group effectively improves the modulus of the system at room temperature, and this rigid structure can maintain the changed shape of the foam when cooled to room temperature. When the foam is heated to 120°C, the material transitions from a glassy state to a high-elastic state. Under external force (flattened or bent into an inverted "V" shape), it is cooled to room temperature while maintaining the external force to retain the temporary shape (flat or inverted "V" shape). When the foam with the temporary shape is placed at 120°C again, it automatically recovers to its initial cylindrical shape within 1 min even after severe twisting deformation. This indicates that the foam DGDHAA/ESO-BAPA exhibits excellent shape memory performance.

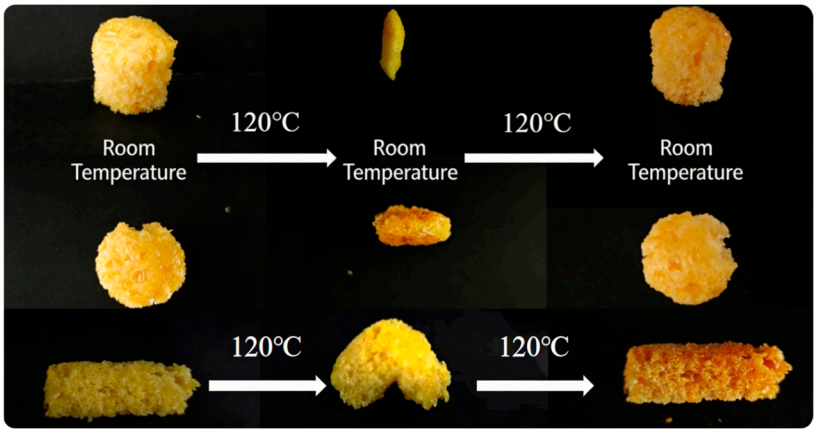

Figure 6: Shape memory performance test of DGDHAA/ESO-BAPA1.0.

3.6 Self-Healing Properties

The significant difference between dynamic polymer networks and traditional covalent networks lies in their inherent self-repairing ability. In traditional covalent networks, the mechanical properties irreversibly decline after damage, while in dynamic networks, the reversible bonds can break and re-form under stimulation, enabling the structural reconstruction and mechanical performance restoration at the damaged site [45]. As shown in Fig. 7, two completely fractured foam pieces were wrapped with tin foil and slightly pressed to ensure intimate interfacial contact, followed by isothermal treatment in an oven at 120°C for 2 h. This temperature condition is not only higher than T_g of the material, which is sufficient to activate the exchange reaction of dynamic covalent bonds, but also avoids the risk of matrix thermal degradation, thereby providing a mild and efficient reaction environment for interfacial healing. During the heating process, the dynamic covalent bonds (hydroxy-ester bonds) at the foam interface underwent a reversible "cleavage-recombination" exchange reaction, forming a continuous three-dimensional cross-linked network. With the extension of reaction time, as the dynamic covalent bond exchange at the interface continued to deepen, the originally distinct fracture interface gradually disappeared, and the two foam pieces were re-fused into an integral whole, restoring the continuous network structure of the original material. The healed foam was suspended with a 500 g weight using a nylon rope, and no secondary fracture occurred, which directly confirmed its excellent self-healing performance. The unique tricyclic phenanthrene rigid skeleton of dehydroabietylamine in the foam endows the cross-linked network with extremely high mechanical

strength and rigidity. After the network at the interface is reconnected, this rigid skeleton enables the entire material to resist significant external tensile force without structural damage. This indicates that the foam DGDHAA/ESO-BAPA exhibits excellent self-healing performance.

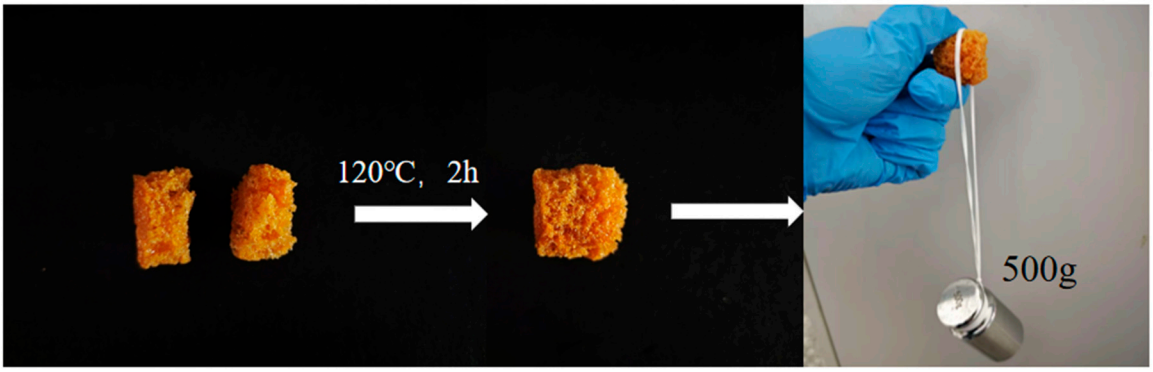

Figure 7: Self-healing performance test of DGDHAA/ESO-BAPA1.0.

3.7 Scanning Electron Microscopy (SEM) Test

Based on the compression performance test results, the DGDHAA/ESO-BAPA 1.0 sample was selected for SEM testing. Fig. 8A shows the SEM image of DGDHAA/ESO-BAPA 1.0. Fig. 8B shows the foam cells are irregular spherical closed-open mixed pores, with pore diameters ranging from 100 μm to 1200 μm, average pore size of 645 μm. White small particles can be seen on the surface of the pore walls, which may be residues of $NaHCO_3$ decomposition products. From the SEM image, the pore size distribution is relatively wide, which is usually related to the mismatch between the decomposition rate of $NaHCO_3$ foaming agent and the gelation rate of the resin. When gas generation proceeds faster than resin curing, the generated gas tends to diffuse and coalesce excessively, thereby producing enlarged pores and a broadened pore size distribution [46,47]. Conversely, slower gas evolution restricts pore growth and tends to form smaller or closed-cell structures. These microscopic observations provide a reliable theoretical basis for the subsequent optimization of foaming conditions and precise regulation of the porous structure of bio-based vitrimer foams.

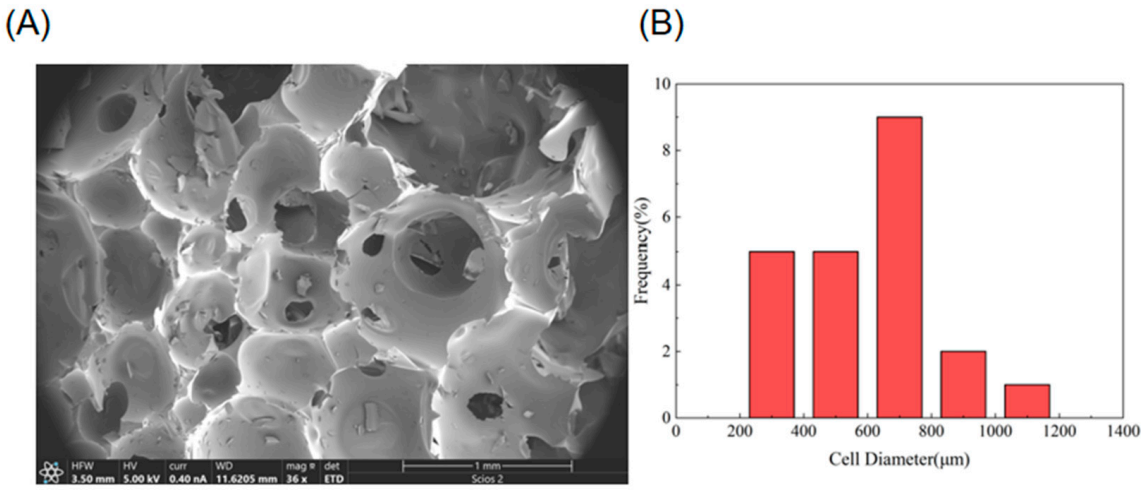

Figure 8: (**A**) SEM images of DGDHAA/ESO-BAPA 1.0. (**B**) the corresponding cell size distribution.

4 Conclusions

A new type of bio-based vitrimer foam was successfully prepared using DGDHAA as the raw material, ESO as the flexibilizer, BAPA as the curing agent, BDMA as the foam stabilizer, and $NaHCO_3$ as the foaming agent. The main research conclusions are as follows: The foam system exhibits good thermal stability with an initial thermal decomposition temperature of approximately 270°C. With the increase of curing agent BAPA content in the system, the crosslinking density increases correspondingly, and the T_g of the material also shows an upward trend, gradually rising from 95.88°C to 98.65°C. Under the appropriate crosslinking density, the foam shows excellent mechanical resilience. Among them, after undergoing 50% compression loading and unloading, the DGDHAA/ESO-BAPA 1.0 sample achieves a rebound rate of 81.84% and can well recover to its original shape. The foam material exhibits a classic "deformation → fixation → recovery" capability at 120°C (above T_g). Its porous micro-skeleton provides sufficient buffer space, effectively avoiding brittle fracture of the material under macro large strain, thereby significantly improving the shape memory performance. Relying on the dynamic covalent bonds in the cross-linked network, after the completely broken foam is treated at a constant temperature of 120°C for 2 h, a dynamic exchange reaction occurs at the interface, realizing the reconnection and healing of the fracture surface. The repaired foam maintains extremely high rigidity and mechanical strength, and can hang a 500 g weight without secondary fracture, achieving an excellent solid-state welding effect. Benefiting from the internal dynamic covalent cross-linking network, the foam fabricated in this study possesses excellent thermal stability. It can be utilized as flame-retardant buffer layers for batteries and diverse thermal insulation components, fully satisfying the sustainable development requirements of green polymer materials. Furthermore, this foam is processable into repairable sports protective gear. Owing to its remarkable self-healing and shape-memory performances, the protective equipment can be repeatedly reshaped and reused, drastically cutting down replacement frequency.

Acknowledgement: Not applicable.

Funding Statement: Financial supports from National Natural Science Foundation of China (32201503), and Funding for School-Level Research Projects of Yancheng Institute of Technology (xjr2022015).

Author Contributions: Wenxuan Zhang: methodology, investigation, writing—original draft, software. Zhengchuang Zhao: investigation, conceptualization. Xiaoting Gao: investigation, conceptualization. Wenning Shen: analysis and interpretation. Ruiqin Deng: formal analysis. Zheng Xing: collecting data. Huimin Cheng: reviewed the manuscript. Xinyan Yan: critical revision of manuscript and Resource. All authors reviewed and approved the final version of the manuscript.

Availability of Data and Materials: The datasets used and analyzed during the current study freely available from the corresponding author on reasonable request.

Ethics Approval: Not applicable.

Conflicts of Interest: The authors declare no conflicts of interest.

Supplementary Materials: The supplementary material is available online at https://www.techscience.com/doi/10.32604/jpm.2026.087801/s1.

References

1. Wang L, Zhang C, Gong W, Ji Y, Qin S, He L. Preparation of microcellular epoxy foams through a limited-foaming process: A contradiction with the time-temperature-transformation cure diagram. Adv Mater. 2018;30(3):1703992. [CrossRef].

2. Tian Y, Feng X, Wang J, Shang S, Liu F, Jiang J, et al. Degradable silver-plated epoxy foams with exceptional Joule heating and electromagnetic shielding properties. Chem Eng J. 2025;508:161065. [CrossRef].
3. Tian Y, Wang P, Wang J, Huang X, Shang S, Jiang J, et al. High-strength and upcyclable bio-based epoxy foams enabled by dynamic networks for multifunctional applications. Chem Eng J. 2026;534:175268. [CrossRef].
4. Jing J, Yao B, Sun W, Chen J, Xu J, Fu J. Ultra-tough, yet rigid and healable supramolecular polymers with variable stiffness for multimodal actuators. Angew Chem Int Ed. 2024:e202410693. [CrossRef].
5. Capelot M, Montarnal D, Tournilhac F, Leibler L. Metal-catalyzed transesterification for healing and assembling of thermosets. J Am Chem Soc. 2012;134(18):7664–7. [CrossRef].
6. Capelot M, Unterlass MM, Tournilhac F, Leibler L. Catalytic control of the vitrimer glass transition. ACS Macro Lett. 2012;1(7):789–92. [CrossRef].
7. Zheng J, Png ZM, Ng SH, Tham GX, Ye E, Goh SS, et al. Vitrimers: Current research trends and their emerging applications. Mater Today. 2021;51:586–625. [CrossRef].
8. Hao Y, Zhong L, Li T, Zhang J, Zhang D. High-performance recyclable and malleable epoxy resin with vanillin-based hyperbranched epoxy resin containing dual dynamic bonds. ACS Sustainable Chem Eng. 2023;11(30):11077–87. [CrossRef].
9. Brown NF, Pradeep SA, Agnihotri S, Pilla S. The power of processing: Creating high strength foams from epoxidized pine oil. ACS Sustainable Chem Eng. 2017;5(10):8641–7. [CrossRef].
10. Altuna FI, Ruseckaite RA, Stefani PM. Biobased thermosetting epoxy foams: Mechanical and thermal characterization. ACS Sustainable Chem Eng. 2015;3(7):1406–11. [CrossRef].
11. Khundamri N, Aouf C, Fulcrand H, Dubreucq E, Tanrattanakul V. Bio-based flexible epoxy foam synthesized from epoxidized soybean oil and epoxidized mangosteen tannin. Ind Crops Prod. 2019;128:556–65. [CrossRef].
12. Li C, Liu X, Zhu J, Zhang C, Guo J. Synthesis, characterization of a rosin-based epoxy monomer and its comparison with a petroleum-based counterpart. J Macromol Sci Part A. 2013;50(3):321–9. [CrossRef].
13. Li T, Liu X, Jiang Y, Ma S, Zhu J. Bio-based shape memory epoxy resin synthesized from rosin acid. Iran Polym J. 2016;25(11):957–65. [CrossRef].
14. Chen C, Li Z, Hu Y, Huang Q, Li X, Qing Y, et al. Rosin acid and SiO_2 modified cotton fabric to prepare fluorine-free durable superhydrophobic coating for oil-water separation. J Hazard Mater. 2022;440:129797. [CrossRef].
15. Colín-Gómez M, Flores-Ramirez N, Vasquez-Garcia SR, García-González L, Domratcheva-Lvova L, Orozco-Cruz R. Synthesis and evaluation of new coatings based on chemically modified rosin and PMMA for steel substrates. Mater Lett. 2022;318:132224. [CrossRef].
16. Yang X, Guo L, Xu X, Shang S, Liu H. A fully bio-based epoxy vitrimer: Self-healing, triple-shape memory and reprocessing triggered by dynamic covalent bond exchange. Mater Des. 2020;186:108248. [CrossRef].
17. Yang R, Tan L, Pan Z, Tian L, Zhang T, Zhao B, et al. High strength, self-activating ability and fast adhesion of polyurethane adhesives based on rosin structure in different environments. Mater Horiz. 2025;12(6):1913–21. [CrossRef].
18. Kugler S, Ossowicz P, Malarczyk-Matusiak K, Wierzbicka E. Advances in rosin-based chemicals: The latest recipes, applications and future trends. Molecules. 2019;24(9):1651. [CrossRef].
19. Kugler S, Wierzbicka E, Ossowicz-Rupniewska P, Łopiński J. Composition and properties of protective coatings made of biologically-derived polyester reactive binder. Polymers. 2021;13(11):1700. [CrossRef].
20. Bei Y, Ma Y, Song F, Kou Z, Hu L, Bo C, et al. Recent progress of biomass based self-healing polymers. J Appl Polym Sci. 2022;139(16):51977. [CrossRef].
21. Lu C, Liu Y, Liu X, Wang C, Wang J, Chu F. Sustainable multiple- and multistimulus-shape-memory and self-healing elastomers with semi-interpenetrating network derived from biomass via bulk radical polymerization. ACS Sustainable Chem Eng. 2018;6(5):6527–35. [CrossRef].
22. Wu Y, Yan C, Wang Y, Gao C, Liu Y. Biomimetic structure of chitosan reinforced epoxy natural rubber with self-healed, recyclable and antimicrobial ability. Int J Biol Macromol. 2021;184:9–19. [CrossRef].
23. Tian Y, Feng X, Wang C, Shang S, Liu H, Huang X, et al. Fully biobased degradable vitrimer foams: Mechanical robust, catalyst-free self-healing, and shape memory properties. ACS Appl Mater Interfaces. 2024;16(5):6523–32. [CrossRef].
24. Huang X, Yang X, Liu H, Shang S, Cai Z, Wu K. Bio-based thermosetting epoxy foams from epoxidized soybean oil and rosin with enhanced properties. Ind Crops Prod. 2019;139:111540. [CrossRef].

25. Chen Y, Tian F, Yao J, Li L, Cui Y, Yang H, et al. Biobased polyurethane adhesives derived from vegetable oil and rosin for flexible packaging applications. ACS Appl Polym Mater. 2024;6(11):6469–81. [CrossRef].
26. Dworakowska S, Cornille A, Bogdał D, Boutevin B, Caillol S. Formulation of bio-based epoxy foams from epoxidized cardanol and vegetable oil amine. Euro J Lipid Sci & Tech. 2015;117(11):1893–902. [CrossRef].
27. Mazzon E, Habas-Ulloa A, Habas JP. Lightweight rigid foams from highly reactive epoxy resins derived from vegetable oil for automotive applications. Eur Polym J. 2015;68:546–57. [CrossRef].
28. Ren Q, Zhu S. One-pack epoxy foaming with CO_2 as latent blowing agent. ACS Macro Lett. 2015;4(7):693–7. [CrossRef].
29. Zhao J, Wang G, Zhang A, Zhao G, Park CB. Nanocellular TPU composite foams achieved by stretch-assisted microcellular foaming with low-pressure gaseous CO_2 as blowing agent. J CO2 Util. 2021;53:101708. [CrossRef].
30. Ren Q, Xu H, Yu Q, Zhu S. Development of epoxy foaming with CO_2 as latent blowing agent and principle in selection of amine curing agent. Ind Eng Chem Res. 2015;54(44):11056–64. [CrossRef].
31. Hussein MS, Teh PL, Rahmat AR, Zainuddin F, Keat YC. The influence of sodium bicarbonate loading as blowing agent on the properties of epoxy foam. Solid State Phenom. 2018;280:270–6. [CrossRef].
32. Li H, Xiao H, Song Y. A preparation method of Ag/AgCl marine electric field electrode with sodium bicarbonate as foaming agent. Mater Lett. 2022;323:132604. [CrossRef].
33. Bethke C, Kaysser ST, Uy Lan DN, Goller SM, van der Zwan KP, Senker J, et al. Synthesis and characterization of dual-functional carbamates as blowing and curing agents for epoxy foam. Ind Eng Chem Res. 2021;60(19):7065–80. [CrossRef].
34. Uy Lan DN, Bethke C, Altstädt V, Ruckdäschel H. Preparation of pros-foam sheets and their epoxy foams using the solid-state carbamate-foaming technique. Polymer. 2022;254:125080. [CrossRef].
35. Chen B, Wang C, Zhang L, Wang C. Synthesis of starch-based polyether non-isocyanate polyurethane with excellent mechanical and foaming properties. Int J Biol Macromol. 2025;330:148147. [CrossRef].
36. Maksym P, Tarnacka M, Dzienia A, Matuszek K, Chrobok A, Kaminski K, et al. Enhanced polymerization rate and conductivity of ionic liquid-based epoxy resin. Macromolecules. 2017;50(8):3262–72. [CrossRef].
37. Liu X, Xin W, Zhang J. Rosin-derived imide-diacids as epoxy curing agents for enhanced performance. Bioresour Technol. 2010;101(7):2520–4. [CrossRef].
38. Song P, Dai J, Chen G, Yu Y, Fang Z, Lei W, et al. Bioinspired design of strong, tough, and thermally stable polymeric materials via nanoconfinement. ACS Nano. 2018;12(9):9266–78. [CrossRef].
39. Garg M, Sharma S, Mehta R. Role of curing conditions and silanization of glass fibers on carbon nanotubes (CNTs) reinforced glass fiber epoxy composites. Compos Interfaces. 2017;24(2):233–53. [CrossRef].
40. Su J, Yang Q, Zhang N, Zhou S, Li R, Hou S, et al. Synergistic effects of thermally induced gradient wettability and pore structure in thermoresponsive polymer-functionalized polyester knitted fabrics for adaptive thermal and moisture regulation. ACS Appl Mater Interfaces. 2025;17(47):64992–5005. [CrossRef].
41. Wang W, Liao X, He Y, Li J, Jiang Q, Li G. Thermoplastic polyurethane/polytetrafluoroethylene composite foams with enhanced mechanical properties and anti-shrinkage capability fabricated with supercritical carbon dioxide. J Supercrit Fluids. 2020;163:104861. [CrossRef].
42. Liu Y, Zhao X, Ye L. A novel elastic urea–melamine–formaldehyde foam: Structure and properties. Ind Eng Chem Res. 2016;55(32):8743–50. [CrossRef].
43. Zhao Q, Qi HJ, Xie T. Recent progress in shape memory polymer: New behavior, enabling materials, and mechanistic understanding. Prog Polym Sci. 2015;49:79–120. [CrossRef].
44. Hu B, Shen S, Zhai M, Zhao N, Huang H, Duan Y, et al. Development of thermoplastic epoxy resin-based multifunctional flexible composite film and its shape memory performance research. Mater Today Commun. 2024;40:109842. [CrossRef].
45. Wang J, Zhou H, Yuan W, Tang J, Yu H, Zhou K, et al. Quadruple H-bond cross-linked polyimide for high temperature resistance, corrosion protection, and self-healing coatings. ACS Appl Polym Mater. 2025;7(17):12053–65. [CrossRef].
46. Jiao L, Xiao H, Wang Q, Sun J. Thermal degradation characteristics of rigid polyurethane foam and the volatile products analysis with TG-FTIR-MS. Polym Degrad Stab. 2013;98(12):2687–96. [CrossRef].
47. Xu Y, Li Y, Hua W, Zhang A, Bao J. Light-weight silver plating foam and carbon nanotube hybridized epoxy composite foams with exceptional conductivity and electromagnetic shielding property. ACS Appl Mater Interfaces. 2016;8(36):24131–42. [CrossRef].